MTJ Magnetization Switching Mechanisms for IoT Applications

Abdelrahman G. Qoutb and Eby G. Friedman
Department of Electrical and Computer Engineering, University of Rochester
Rochester, New York 14627
a.qoutb@rochester.edu, friedman@ece.rochester.edu

ABSTRACT

Different magnetization mechanisms, structures, and electrical properties of MTJ-based MRAM are described in the context of IoT applications. MTJ-based MRAM provides non-volatility (high retention time), low power, and high speed. This memory has a broad variety of applications. One important example is IoT. A comparative study of the magnetization mechanisms provides insight into which MTJ structures and magnetization mechanisms best support different IoT applications.

ACM Reference format:

A. G. Qoutb and E. G. Friedman. 2018. MTJ Magnetization Switching Mechanisms for IoT Applications. In *Proceedings of ACM Great Lakes Symposium on VLSI, Chicago, Illinois, USA, May 23-25, 2018 (GLSVLSI'18)*, 6 pages.
DOI: http://dx.doi.org/10.1145/3194554.3194624

1 INTRODUCTION

The internet of things (IoT) or the internet of everything has become a primary vehicle for connecting multiple nodes throughout a large network. Each of these nodes may include a small processing unit to collect information, communicate with other nodes, and respond to stimuli. Integrated memory will be needed in all of these IoT applications. Form factor, initialization time, power dissipation, read/write speed, and cost are primary design criteria. Magnetic tunnel junction (MTJ)-based magnetic random access memory (MRAM) is a potentially important solution for IoT applications. MTJ-based MRAM provides a nonvolatile memory able to operate at low latency, low leakage current, and high density. These capabilities support MRAM becoming the universal memory as compared to other nonvolatile memories such as e-Flash, phase change RAM, or resistive RAM [1].

This discussion is outlined as follows. In section 2, the physical behavior and parameters affecting MTJ device performance are described. Different forms of magnetization operation are also discussed in section 2. In section 3, the primary magnetization mechanisms for different structures are characterized. A comparative study of the different magnetization mechanisms described in section 3 is provided in section 4, emphasizing scaling, power dissipation, and circuit speed. A discussion of the effects of thermal variations on the different magnetization mechanisms for IoT applications is provided in section 5. Appropriate magnetization mechanisms applicable for different IoT applications are also described in sections 4 and 5. A summary is provided in the conclusions section.

2 MTJ STRUCTURES FOR MRAM

Tunneling magnetoresistance (TMR) was discovered in 1975 by Julliere [2] within a structure called a magnetic tunnel junction. It was not until the mid-1990s when fabrication of reliable MTJs became possible with the development of certain growth techniques and lithographic processes [3,4] did MTJ become a commercially interesting technology. The basic MTJ structure is composed of two ferromagnetic (FM) materials separated by a nonmagnetic insulator, where the conductivity of the structure is determined by the angle between the magnetization direction of the two ferromagnetic layers. Maximum conductivity is achieved when both magnetization directions are in parallel, and minimum conductivity when anti-parallel (AP). Slonczewski describes the conductance of the structure as a function of θ, the angle between the magnetization direction in the two FM materials, as [5]

$$G(\theta) = G_o(1 + P^2 cos\ \theta), \quad (1)$$

where P is the spin polarization of the ferromagnetic/barrier couple, and G_o is the conductance of the AP configuration. A primary parameter characterizing the quality of an MTJ is the *TMR*,

$$TMR = \frac{G_P - G_{AP}}{G_{AP}}, \quad (2)$$

where G_P and G_{AP} are, respectively, the conductivity of the parallel ($\theta = 0^o$) and anti-parallel ($\theta = 180^o$) configurations.

This research is supported in part by the National Science Foundation under Grant No. CCF-1329374, CCF-1526466, and CCF-1716091, IARPA under Grant No. W911NF-14-C-0089, AIM Photonics under Award No. 059447-007, the Intel Collaborative Research Institute for Computational Intelligence (ICRI-CI), Singapore Ministry of Education Tier 2 under Grant No. MOE2014-T2-2-105, and by grants from Cisco Systems, Qualcomm, and 0eC.

GLSVLSI'18, May 23-25, 2018, Chicago, IL, USA.

ACM ISBN 978-1-4503-5724-1/18/05...$15.00.
DOI: http://dx.doi.org/10.1145/3194554.3194624

The ability to control the MTJ conductivity by the difference in magnetization angle θ is the key concept in using an MTJ as a building block for magnetic memory (such as MRAM). The FM layer is pinned while controlling the direction of magnetization of the other FM free layer (the storage layer). The FM layers are fabricated as uniaxial anisotropy layers (with a preferable single magnetization axis). The magnetization dynamics in the free layer are derived from the Landau–Lifshitz–Gilbert (LLG) equation [6,7], as

$$\frac{\partial M}{\partial t} = -\gamma M \times H_{eff} + \alpha M \times \frac{\partial M}{\partial t} - \gamma \Sigma \tau_i , \quad (3)$$

where $\vec{M}$ is the free layer magnetization, t is the time variable, $\vec{H}_{eff}$ is the effective magnetic field applied to the free layer, γ is the gyromagnetic ratio, α is the Gilbert damping factor, and $\vec{\tau}_i$ is the applied torque due to other switching mechanisms such as spin transfer torque (STT) or spin orbital torque (SOT). The effective magnetic field applied to the free layer $\vec{H}_{eff}$ is [8]

$$H_{eff} = H_{UA} - H_{dem} + H_c + H_{APP} - H_{VCMA} + H_{th} , \quad (4)$$

where $\vec{H}_{UA}$ is the uniaxial anisotropy field, $\vec{H}_{dem}$ is the demagnetization field, $\vec{H}_c$ is the coupling field due to the other FM layer, $\vec{H}_{APP}$ is the applied magnetic field, $\vec{H}_{VCMA}$ is due to the voltage controlled magnetic anisotropy (VCMA), and $\vec{H}_{th}$ is the stochastic magnetic field due to thermal variations.

MTJ structures are based on uniaxial anisotropy which means the magnetization direction prefers stability over a single axis (easy axis), ensuring the free layer is either in the parallel state or antiparallel state with respect to the pinned reference layer. Switching is controlled by applying a perturbing field by injecting current, applying an external magnetic field, or some other means. Uniaxial magnetic anisotropy (MA) is achieved by different MTJ structures to obtain either an in-plane MTJ (IMTJ) or perpendicular MTJ (PMTJ). Shape magnetic anisotropy is the main source for in-plane magnetic anisotropy where an elliptical MTJ is preferred as the magnetization tends to be directed along the long axis. A circular shape is preferred in the case of a perpendicular MTJ (PMTJ). Perpendicular magnetic anisotropy (PMA) in a PMTJ is due to two reasons, magneto-crystalline anisotropy of the crystalline lattice of the FM layer or by an interfacial magnetic anisotropy due to coupling at the interface between the FM layer and a neighboring layer (such as Co/Pt and Co/Pd [9]).

The pinned reference FM layer is achieved through the exchange bias effect by attaching an FM layer to an antiferromagnetic material. A synthetic antiferromagnetic structure (SAF) is preferred to achieve the pinned FM layer by using two antiparallel FM layers separated by a nonmagnetic (NM) metallic layer, reducing any stray fields affecting the free layer, as shown in Figure 1.

Numerous developments in MTJ structures have been achieved to enhance the TMR and other performance metrics. Different configurations used to switch the MTJ magnetization are discussed in section 3. Switching by applying a magnetic field or injecting a current through the MTJ structure is described. Other forms of assistive switching, such as thermally assisted switching, are also discussed.

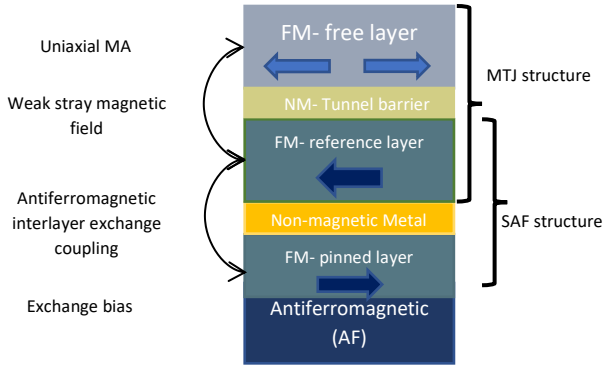

Figure 1. Stacking structure of IMTJ with SAF

3 MTJ-BASED MRAM MAGNETIZATION MECHANISMS

Several magnetization mechanisms of MTJ-based MRAM have been developed. Controlling the magnetization direction of the free layer can be achieved by applying an external magnetic field (induced by current passing through a nearby wire) [10], injecting current through an MTJ structure to cause thermal perturbations to affect device magnetization properties (thermally assisted) [11], injecting greater current to induce spin transfer torque to the magnetization layer [12], or by adding an additional perpendicular magnetization layer within an IMTJ to enhance STT performance to reduce the write current [13]. Recently developed magnetization mechanisms in MRAM are also discussed in this section.

3.1 Field-Induced Magnetic Switching MRAM (FIMS-MRAM)

The magnetic field required to switch an MTJ is governed by the relationship, $\mu_o H_{write} = 2K/M_s$, where K is a constant characterizing the magnetic anisotropy of the MTJ. The Stoner-Wohlfarth MRAM (ST-MRAM) was the first demonstrated MTJ-based MRAM, based on Stoner-Wohlfarth (SW) switching, as shown in Figure 2 [14]. Two orthogonal magnetic fields - one along the easy axis - are applied to an MTJ structure. The total field applied over the x and y axis, respectively, H_x and H_y, based on (5), sets the lower limit of the write field,

$$H_x^{2/3} + H_y^{2/3} = \left(\frac{2K_u}{M_s}\right)^{2/3}, \quad (5)$$

where K_u is the magnetic anisotropy constant and M_s is the saturated magnetization. The upper limit of the switching operation is bounded by the MTJ shape, where the easy axis field is lower than the anisotropy field, $H_K = 2K_u/M_s$.

An improved field written mechanism has been achieved by Savtchenko [15], where two orthogonal fields are oriented at an angle of 45^o to the MTJ easy axis. The write operation is performed in a toggle form to maintain full magnetization operation, hence called "Toggle MRAM." The spin flip flop field H_{spin_flop} is

$$\mu_o M_s H_{spin\_flop} = 2\sqrt{K_{eff}\left(\frac{A}{t} + K_{eff}\right)}, \quad (6)$$

assuming the two FM layers are identical with a thickness t (a symmetric MTJ). K_{eff} is the effective anisotropy, and A is the interfacial coupling through the spacer (the tunnel barrier).

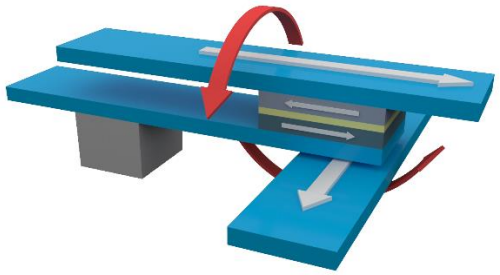

Figure 2. IMTJ writing using FIMS

3.2 Spin Transfer Torque MRAM (STT-MRAM)

In STT-MRAM, switching the magnetization of the free layer is achieved by passing a polarized electric current through an MTJ structure, where the polarized moving electrons exert a torque on the magnetic storage layer. When a normal unpolarized current passes through an FM layer, the current becomes polarized by the FM layer with a spin polarization factor [5]. Based on whether the current direction is into or out of the MTJ structure (the pinned layer), respectively, an antiparallel or parallel configuration is achieved, as shown in Figure 3.

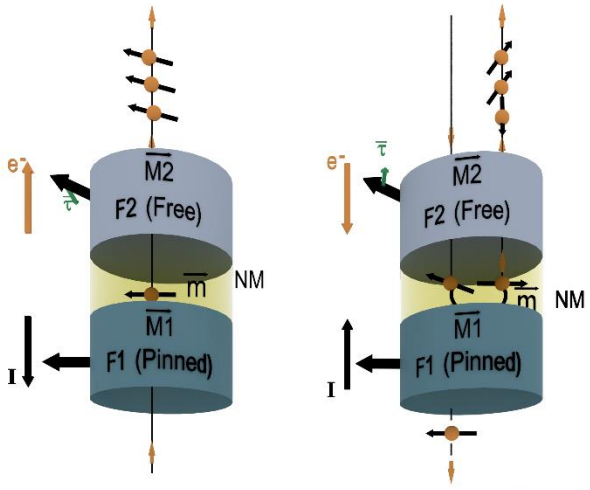

Figure 3. IMTJ writing using STT

The switching current should be greater than a critical magnitude, where the level depends upon the device dimensions and materials. For an IMTJ, the critical current density J_{co} to switch the FM layer is described by (8). The critical current is affected by thermal variations and depends upon the width of the current pulse. The critical current $J_c(t)$ is described by (7),

$$J_c(t) = J_{co}\left[1 - \frac{K_B T}{K_u V_{FL}} ln\left(\frac{t}{\tau_o}\right)\right], \quad (7)$$

$$J_{co} = \frac{2e\alpha\mu_o M_s t_{FL}(H_{K\parallel}+(\frac{M_s}{2}))}{\hbar\eta}, \quad (8)$$

where e is the electron charge, μ_o is the permeability of free space, t_{FL} is the thickness of the FM, $H_{K\parallel}$ is the in-plane magnetic anisotropy field, $\hbar$ is the reduced plank constant, η is the spin transfer efficiency, t is the pulse width, K_B is the Boltzmann constant, T is the temperature, K_u is the uniaxial magnetic anisotropy constant, V_{FL} is the volume of the FM layer, and $\tau_o \sim 1$ is the inverse of the frequency factor or the attempt frequency of the thermal reaction.

For an IMTJ, the magnetization configuration does not efficiently support both thermal stability and writability [8]. Other configurations to reduce the critical current in an IMTJ are

- Dual MTJ: where the storage FM layer is sandwiched between two pinned FM layers, hence the current passing through the structure exerts a larger torque (2x), reducing the critical current to switch the layer [16].
- Perpendicular polarizer: where a perpendicular polarizer is stacked within an MTJ [17], enhancing the precessional switching. The storage layer acquires an out-of-plane component due to the added magnetic precessional movement.
- Reduced demagnetized field: where either volume or interfacial perpendicular magnetic anisotropy is added – by changing the barrier and FM materials – decreasing the demagnetizing field effect, thereby reducing the critical current [18].

MTJ structures that exhibit magnetic anisotropy normal to the surface are faster, dissipate less power, and are higher density than an IMTJ due to a lower critical current and the circular shape of the magnetic cell. A PMTJ-based MRAM is therefore more appropriate for IoT applications than an IMTJ. The critical current density J_{co} for a PMTJ is described by (9) where $H_{K\perp}$ is the perpendicular-to-plane magnetic anisotropy,

$$J_{co} = \frac{2e\alpha\mu_o M_s t_{FL}(H_{K\perp} - M_s)}{\hbar\eta}. \quad (9)$$

A PMTJ suffers from a higher Gilbert damping factor α than an IMTJ. In addition, it is difficult to fabricate the crystalline PMTJ structure to produce perpendicular magnetic anisotropy. The critical procedures of annealing and oxidation are required to grow a PMTJ. That leads to a preferential choice between IMTJ and PMTJ based on the manufacturing difficulty. A comparative study between IMTJ and PMTJ in terms of IoT applications is provided in section 4.

3.3 Thermally assisted MRAM (TA-MRAM)

In TA-MRAM, thermal variations are induced by passing current through an MTJ and/or using a high thermal conductivity material. The magnetic anisotropy constant is lower at higher temperatures which affects the magnetic field writing to the storage layer. Accordingly, a thermal assist mechanism is integrated within the FIMS-MRAM structure, achieving higher performance [19].

The same concept can be applied to an STT-MRAM, where the same current line is used for heating and switching the cell. The write operation is composed of multiple stages. The first stage

heats the cell by passing a current for a specific duration. A lower level of current is applied for a different duration to switch the state. The cell is left to cool, storing the written state [20].

4 COMPARATIVE STUDY

A PMA-based STT-MRAM structure exhibits better performance, as listed in Table 1, due to a higher density and reduced power [21]. Research is on-going for determining the optimum device characteristics to provide acceptable performance as a replacement memory technology. Research on different structures, materials, and mechanisms suggests that a PMTJ-based MRAM is more applicable for those IoT applications that require higher operating speed.

Table 1. Advantages and disadvantages of different MTJ structures

Technique	Advantages	Disadvantages
IMA	• Controlled retention time	• Density, power consumption
Interfacial PMA	• Higher density • Optimizing I_c and α	• Low retention time
Crystalline PMA	• Higher density	• Larger α • Low retention time
SAF pinned layer	• Symmetric MTJ switching	• Increases height of MTJ stack
Dual MgO/Free layer interface	• Enhance interfacial PMA • Reduces α	• Increases MTJ resistance ($R_{\|MTJ}$)
Dual tunnel barrier with dual PL	• Reduces I_c, α	• Increases $R_{\|MTJ}$ • Increases height of MTJ stack
Tilted magnetic anisotropy(MA)	• Reduces I_c	• Reduces TMR ratio • Difficult to fabricate
Orthogonal pinned layer	• Reduces I_c without affecting TMR ratio	• Increases height of MTJ stack • Difficult to fabricate

A comparison of magnetization mechanisms for MTJ-based MRAM is summarized in Table 2 [22,1]. A FIMS-MRAM is based on an IMTJ, requiring large cells (which suffers from scaling and bit selectivity due to stray field disturbance from the writing magnetic field from neighboring cells). FIMS consumes large power (due to the large write current to induce the write magnetic field) but exhibits long retention times and thermal stability.

Toggle based MRAM solves the selectivity problem but can place the memory bit in an undefined state – requiring the read operation to be performed before the write operation. A toggle MRAM is predicted to not be highly scalable below 90 nm [1]. FIMS is a robust technology, exhibiting high reliability, endurance, and resistance to radiation, making it a good candidate for automotive, sensor-based weather forecasting, and IoT applications [8,25].

Table 2. Performance of different magnetization mechanisms

	Scalability	Endurance	Write time	Write current
FIMS	Poor	10^{16}	>10 ns	~ 10 mA
Toggle	Good	10^{15}	>30 ns	>30 mA
TAS	Good	10^{12}	>20 ns	~ 1 mA
STT	Very good	10^{16}	<5 ns	~100 µA
TAS+STT	Best	10^{12}	<8 ns	~100µA

The advantages and disadvantages of STT-MRAM are illustrated in Figure 4 [24], where the reliability is improved by optimizing the read/write currents, utilizing novel FM and barrier materials, or applying different magnetization mechanisms such as VCMA or SOT. Spin orbit torque MRAM (SOT-MRAM) shows promising potential due to the separate read and write paths, supporting symmetric switching.

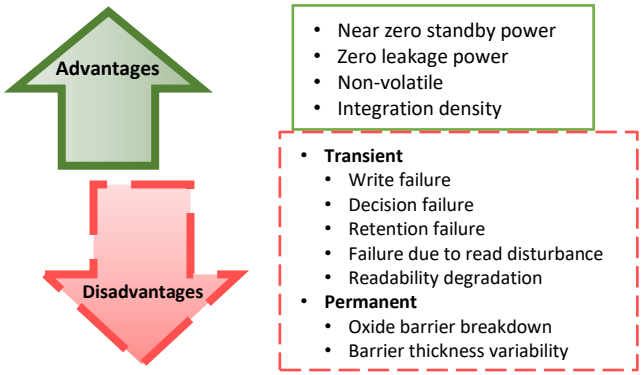

Figure 4. Advantages and reliability challenges of STT-MRAM

The thermally assisted switching (TAS) mechanism requires less writing power and is higher speed than FIMS, although difficult to scale. STT-based mechanisms exhibit better performance for both IMTJ and PMTJ [1,21-24]. TAS-based MRAM suffers from the same problems as FIMS. Merging TAS with STT-MRAM exhibits better scalability and performance as compared to FIMS, TAS, and STT-MRAM [22,1]. TAS+STT-MRAM is a good candidate for IoT applications which require high speed while dissipating low power.

5 MTJ-BASED MRAM FOR DIFFERENT TEMPERATURES

The operation of an MTJ-based MRAM as a nonvolatile memory is composed of three states. The write state with one magnetization mechanism, the retention state, describing how long the memory can maintain the written information, and the read state. The key objective in MTJ-based MRAM is to maintain low read/write/idle power consumption, high retention time, a wide operating temperature range, and low read and write delays. Each of these objectives are affected by the thermal stability factor Δ, as expressed in (10),

$$\Delta = \frac{\Delta E}{K_B T} = \frac{\mu_o {M_s}^2 {t_{FL}}^2 (A_R - 1) w}{K_B T}\Big|_{IMTJ} = \frac{[(K_v - (1/4)\mu_o (3N_z - 1){M_s}^2) t_{FL} + K_s]\frac{\pi}{4} w^2}{K_B T}\Big|_{PMTJ}, \quad (10)$$

where $\Delta E = K_{eff} V_{FL}$ is the barrier height of the magnetic material. For an elliptically shaped FM IMTJ layer, A_R is the aspect ratio of the ellipse with width w. A circular FM PMTJ layer has a diameter w, K_v is the PMA constant, K_s is the surface energy, and N_z is the perpendicular-to-plane demagnetization coefficient.

The thermal stability factor decreases with scalability, as shown in (10), directly affecting the retention time and power consumption. The integration density, error rate, and thermal stability of MTJs are presented in [26], as shown in Figure 5, describing the critical integration level while maintaining an acceptable error rate.

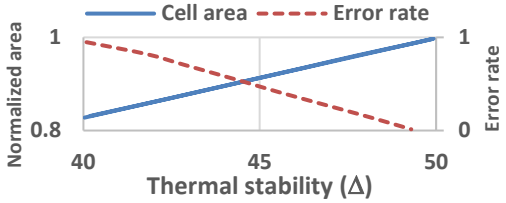

Figure 5. Impact of thermal stability on cell area and error rate

Thermal variations affect the electrical device characteristics (K_{eff}, J_{co}, TMR) in a stochastic manner. TMR was discovered in a Fe-GeO-Co structure at 4.2 K [2]. By the mid-1990s, a *TMR* ratio of 10 to 70% at room temperature was achieved [3], [4]. Later, after 2004, giant TMR exhibited a ratio of 250% - reaching up to 600% - at room temperature by using a monocrystalline magnesium oxide (MgO) barrier [27–29]. These developments achieve a PMTJ with perpendicular anisotropy with low switching current and high thermal stability [22,30] which is appropriate for ultra-low power sensor nodes used in IoT applications. Toggle MRAM exhibits a wide range of operating temperatures, from 0 to 70°C for commercial applications [19,28] and −40 to 125°C for automotive and military applications. These different operating temperatures are particularly relevant for IoT-based sensor nodes and processing units located in extreme environmental conditions.

6 MTJ-BASED MRAM FOR DIFFERENT IoT APPLICATIONS

Wireless sensor networks are a form of IoT, where the sensors are located at far distances and operate autonomously and for a long time. The nodes are expected to survive extreme environmental conditions while conserving energy. The sensor node behaves as an embedded system where an operating system is located within local memory. More than ten year retention time is a useful capability for those memories supporting IoT systems. Retention time, power consumption, and thermal stability are directly proportional to the current levels (which is proportional to the size of the MTJ), as described in Table 3 for STT-MRAM [31].

Table 3. Retention time versus write latency for STT-MRAM

Retention Time	10 ms	1 sec	10 years
Write Latency (ns)	3	6	11
I_c (μA)	61	82	114

MRAM with different magnetization mechanisms has been integrated into commercial applications, as shown in Figure 6 [30]. Everspin Technologies recently released a 1 Gb DDR4 Spin Torque MRAM. GlobalFoundries and eVaderis announced the development of an ultra-low power microcontroller based on an embedded magnetoresistive non-volatile memory.

MRAM provides a fast write-read and low power consumption with no static power which positions this technology for many IoT applications. For those IoT applications which require intermittent access with fast working memory, TAS with STT-MRAM is a good candidate, while greater development is needed to enhance read access and read failure rates.

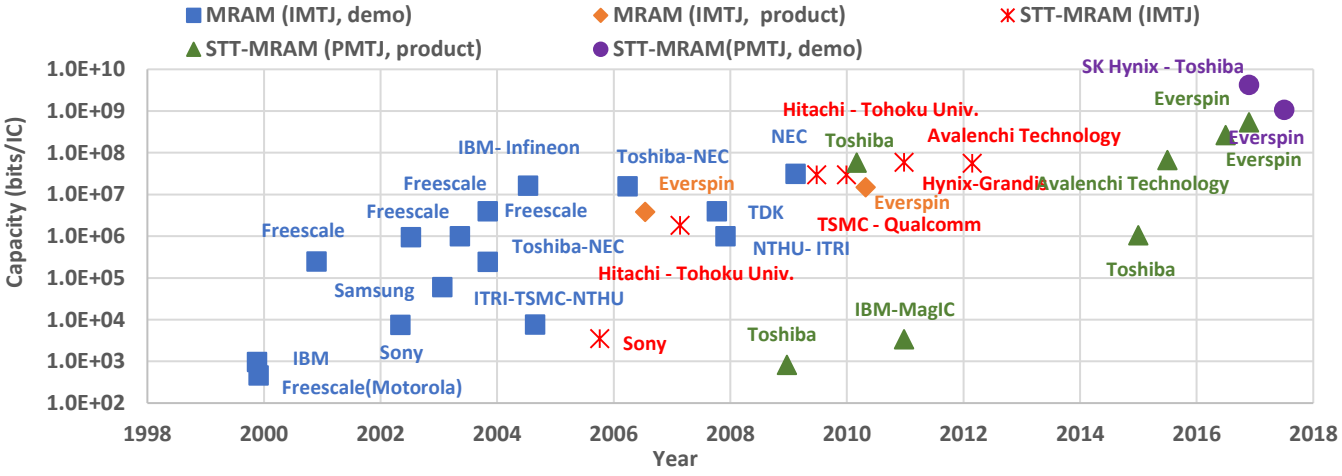

Figure 6. MRAM development trend

Toggle MRAM is a good candidate for those IoT applications requiring long periods of standby current as this technology is non-volatile with fast write times. TAS with STT-MRAM within a PMTJ structure is a better choice for ultra-low power, battery operated IoT nodes, as this application requires zero standby energy with a fast power-up time.

6 CONCLUSIONS

MTJ-based MRAM is an effective candidate technology for the specialized memory needed in IoT applications. PMTJ structures exhibit higher density and lower power than IMTJ due to the circular shape and perpendicular interfacial or magnetocrystalline anisotropy. STT-MRAM assisted with TAS provides enhanced speed and power as compared to FIMS, toggle, TAS, and STT-MRAM. The ability to maintain a ten year retention time operating at extremely low energy makes MRAM highly appropriate for IoT applications, particularly for sensor nodes located in harsh environmental conditions.

REFERENCES

[1] S. Senni, *et al.*, "Exploring MRAM Technologies for Energy Efficient Systems-On-Chip," *IEEE Journal on Emerging and Selected Topics in Circuits and Systems*, Volume 6, No. 3, pp. 279–292, September 2016.

[2] M. Julliere, "Tunneling Between Ferromagnetic Films," *Physics Letters A*, Volume 54, No. 3, pp. 225–226, September 1975.

[3] T. Miyazaki and N. Tezuka, "Giant Magnetic Tunneling Effect in Fe/Al2O3/Fe Junction," *Journal of Magnetism and Magnetic Materials*, Volume 139, No. 3, pp. L231–L234, January 1995.

[4] J. S. Moodera, L. R. Kinder, T. M. Wong, and R. Meservey, "Large Magnetoresistance at Room Temperature in Ferromagnetic Thin Film Tunnel Junctions," *Physical Review Letters*, Volume 74, No. 16, pp. 3273–3276, April 1995.

[5] J. C. Slonczewski, "Current-Driven Excitation of Magnetic Multilayers," *Journal of Magnetism and Magnetic Materials*, Volume 159, No. 1–2, pp. L1–L7, June 1996.

[6] T. L. Gilbert and H. Ekstein, "Basis of the Domain Structure Variational Principle," *The Bulletin of the American Physical Society*, Volume 1, p. 25, 1956.

[7] T. L. Gilbert, "Classics in Magnetics a Phenomenological Theory of Damping in Ferromagnetic Materials," *IEEE Transactions on Magnetics*, Volume 40, No. 6, pp. 3443–3449, November 2004.

[8] B. Dieny, R. B. Goldfarb, and K.-J. Lee, *Introduction to Magnetic Random-Access Memory*. Wiley-IEEE Press, 2016.

[9] K. Yakushiji, *et al.*, "Ultrathin Co/Pt and Co/Pd Superlattice Films for MgO-Based Perpendicular Magnetic Tunnel Junctions," *Applied Physics Letters*, Volume 97, No. 23, p. 232508, December 2010.

[10] R. Patel, *et al.*, "Reducing Switching Latency and Energy in STT-MRAM Caches With Field-Assisted Writing," *IEEE Transactions on Very Large Scale Integration (VLSI) Systems*, Volume 24, No. 1, pp. 129–138, January 2016.

[11] I. L. Prejbeanu, *et al.*, "Thermally Assisted MRAM," *Journal of Physics: Condensed Matter*, Volume 19, No. 16, p. 165218, April 2007.

[12] A. V Khvalkovskiy, *et al.*, "Basic Principles of STT-MRAM Cell Operation in Memory Arrays," *Journal of Physics D: Applied Physics*, Volume 46, No. 7, p. 74001, February 2013.

[13] H. Liu, *et al.*, "Ultrafast Switching in Magnetic Tunnel Junction Based Orthogonal Spin Transfer Devices," *Applied Physics Letters*, Volume 97, No. 24, p. 242510, December 2010.

[14] E. C. Stoner and E. P. Wohlfarth, "A Mechanism of Magnetic Hysteresis in Heterogeneous Alloys," *Philosophical Transactions of the Royal Society A: Mathematical, Physical and Engineering Sciences*, Volume 240, No. 826, pp. 599–642, May 1948.

[15] S. Leonid, *et al.*, "Method of Writing to Scalable Magnetoresistance Random Access Memory Element," U.S. Patent No. 6,545,906B1, October 2001.

[16] Z. Diao, *et al.*, "Spin Transfer Switching in Dual MgO Magnetic Tunnel Junctions," *Applied Physics Letters*, Volume 90, No. 13, p. 132508, March 2007.

[17] D. Houssameddine, *et al.*, "Spin-Torque Oscillator Using a Perpendicular Polarizer and a Planar Free Layer," *Nature Materials*, Volume 6, No. 6, pp. 447–453, June 2007.

[18] S. Mangin, *et al.*, "Current-Induced Magnetization Reversal in Nanopillars with Perpendicular Anisotropy," *Nature Materials*, Volume 5, No. 3, pp. 210–215, March 2006.

[19] J. Wang and P. P. Freitas, "Low-Current Blocking Temperature Writing of Double Barrier Magnetic Random Access Memory Cells," *Applied Physics Letters*, Volume 84, No. 6, pp. 945–947, February 2004.

[20] E. Gapihan, *et al.*, "FeMn Exchange Biased Storage Layer for Thermally Assisted MRAM," *IEEE Transactions on Magnetics*, Volume 46, No. 6, pp. 2486–2488, June 2010.

[21] X. Fong, *et al.*, "Spin-Transfer Torque Memories: Devices, Circuits, and Systems," *Proceedings of the IEEE*, Volume 104, No. 7, pp. 1449–1488, July 2016.

[22] H. Cai, *et al.*, "Exploring Hybrid STT-MTJ/CMOS Energy Solution in Near-/Sub-Threshold Regime for IoT Applications," *IEEE Transactions on Magnetics*, Volume 54, No. 2, pp. 1–9, February 2018.

[23] R. De Rose, *et al.*, "Impact of Voltage Scaling on STT-MRAMs through a Variability-Aware Simulation Framework," *Proceedings of the International Conference on Synthesis, Modeling, Analysis and Simulation Methods and Applications to Circuit Design*, pp. 4–7, June 2017.

[24] S. Salehi, D. Fan, and R. F. Demara, "Survey of STT-MRAM Cell Design Strategies: Taxonomy and Sense Amplifier Tradeoffs for Resiliency," *ACM Journal on Emerging Technologies in Computing Systems*, Volume 13, No. 3, pp. 1–16, April 2017.

[25] J. Heidecker, "MRAM Technology Status: NASA Electronic Parts and Packaging (NEPP) Program Office of Safety and Mission Assurance," Pasadena, California, February 2013.

[26] B. Del Bel, *et al.*, "Improving STT-MRAM Density through Multibit Error Correction," *Proceedings of the IEEE Design, Automation & Test in Europe Conference*, pp. 1–6, March 2014.

[27] S. S. P. Parkin, *et al.*, "Giant Tunnelling Magnetoresistance at Room Temperature with MgO (100) Tunnel Barriers," *Nature Materials*, Volume 3, No. 12, pp. 862–867, December 2004.

[28] S. Yuasa, *et al.*, "Giant Room-Temperature Magnetoresistance in Single-Crystal Fe/MgO/Fe Magnetic Tunnel Junctions," *Nature Materials*, Volume 3, No. 12, pp. 868–871, December 2004.

[29] S. Ikeda, *et al.*, "Tunnel Magnetoresistance of 604% at 300K by Suppression of Ta Diffusion in CoFeB/MgO/CoFeB Pseudo-Spin-Valves Annealed at High Temperature," *Applied Physics Letters*, Volume 93, No. 8, p. 82508, August 2008.

[30] S. Ikeda, *et al.*, "Recent Progress Of Perpendicular Anisotropy Magnetic Tunnel Junctions for Nonvolatile VLSI," *SPIN*, Volume 2, No. 3, p. 1240003, September 2012.

[31] A. Jog, *et al.*, "Cache Revive: Architecting Volatile STT-RAM Caches for Enhanced Performance in CMPs," *Proceedings of the IEEE/ACM Design Automation Conference*, pp. 243-252, June 2012.